Eur Biophys J (2009) 38:447–456
DOI 10.1007/s00249-008-0390-0

ORIGINAL PAPER

FLIM and emission spectral analysis of caspase-3 activation inside single living cell during anticancer drug-induced cell death

Wenliang Pan · Junle Qu · Tongsheng Chen · Lei Sun · Jing Qi

Received: 18 September 2008 / Revised: 5 December 2008 / Accepted: 7 December 2008 / Published online: 9 January 2009

Abstract Two-photon excitation (TPE) fluorescence lifetime imaging microscopy (FLIM) and emission spectral imaging (ESI) are powerful tools for fluorescence resonance energy transfer (FRET) measurement. In this study, we use these two techniques to analyze caspase-3 activation inside single living cells during anticancer drug-induced human lung adenocarcinoma (ASTC-a-1) cell death. TPE-ESI of SCAT3, a caspase-3 indicator based on FRET, was performed inside single living cell stably expressing SCAT3. The TPE-ESI measurement was performed using 780 nm excitation which was considered to selectively excite the donor ECFP of SCAT3 by measuring the emission ratio of 526 to 476 nm. The emission peak at 526 nm disappeared and that of 476 nm increased after STS or bufalin treatment, but taxol treatment did not induce a significant change for the SCAT3 emission spectra, indicating that caspase-3 was activated during STS- or bufalin-induced cell apoptosis, but was not involved in taxol-induced PCD. Fluorescence lifetime of ECFP inside living cells was acquired using FLIM. The lifetime of ECFP was the same as that of the control group after taxol treatment, but increased from 1.83 ± 0.02 to 2.05 ± 0.03 and 1.90 ± 0.03 ns, respectively after STS and bufalin treatment, which agree with the results obtained using TPE-ESI. Taken together, TPE-FLIM and ESI analysis were proved to be valuable approaches for monitoring caspase-3 activation inside single living cells.

Keywords FLIM · Emission spectra · FRET · Caspase-3 · Anticancer drug · Programmed cell death (PCD)

Abbreviations

ASTC-a-1 cell	Human adenocarcinoma cell
ECFP	Enhanced cyan fluorescent protein
EYFP	Enhanced yellow fluorescent protein
ESI	Emission spectral imaging
FLIM	Fluorescence lifetime imaging microscopy
FRET	Fluorescence resonance energy transfer
PCD	Programmed cell death
STS	Staurosporine
SCAT3	A sensor for activated caspase-3 based on FRET
TPE	Two-photon excitation
Venus	Mutation of EYFP

Introduction

Apoptosis, one of the programmed cell death (PCD), is a highly ordered form of cell suicide (Kerr et al. 1994). The biochemical apoptosis is activated via two well-established pathways: death receptor-mediated pathway and mitochondria-mediated pathway. Both of these pathways converge on the activation of downstream executioner caspase-3 (Green 1998), which leads to the biochemical and morphological changes that are characteristic of apoptosis including cell shrinkage, chromatin condensation, DNA

W. Pan and J. Qu contributed equally to this study.

W. Pan · T. Chen (✉) · L. Sun
MOE Key Libratory of Laser Life Science and Institute of Laser Life Science, South China Normal University, 510631 Guangzhou, China
e-mail: chentsh@scnu.edu.cn

J. Qu · J. Qi
Institute of Optoelectronics, Key Laboratory of Optoelectronic Devices and Systems of Ministry of Education, Shenzhen University, 518060 Shenzhen, Guangdong Province, China

fragmentation, and the formation of membrane-enclosed apoptotic bodies containing well-preserved organelles (Kerr et al. 1994; Sun et al. 1999). Staurosporine (STS), which was usually used as a positive control on caspase-3 activation study (Salako et al. 2006; Rehm et al. 2002), is known to be a powerful inducer of apoptosis in a variety of cell types (Andersson et al. 2000; Xue et al. 2003). Bufalin, one of the components of bufadienolides in the traditional Chinese medicine Chan'su, selectively inhibits the growth of various lines of human tumor cells, such as leukemia (Masuda et al. 1995; Watabe et al. 1998) and prostatic cancer (Yeh et al. 2003) by inducing apoptosis. Taxol, a chemotherapeutic agent, exhibits abroad spectrum in clinical activity against human cancers (Day et al. 2006; Shajahan et al. 2007). Although most reports showed a requirement for caspase activation in taxol-induced PCD (Ling et al. 2001; Lu et al. 2005; Son et al. 2006), caspase-independent mechanism(s) was also suggested (Chen et al. 2008; Huisman et al. 2002; Ofir et al. 2002; Wang et al. 2008).

Fluorescence resonance energy transfer (FRET) microscopy has been widely used in the study of protein–protein interactions inside intact living cells (Lin et al. 2006; Rosales et al. 2007; Wan et al. 2008; Wu et al. 2007; Zhang et al. 2008). FRET is a quantum mechanical process between two fluorophores whereby energy from an excited donor molecule is transferred to the acceptor molecule by means of a near-field dipole–dipole coupling (Förster 1948). FRET can only occur when the distance between the donor and acceptor is less than about 10 nm, and the emission spectrum of the donor largely overlaps with the absorption spectrum of the acceptor. The efficiency of FRET is dependent on the inverse sixth power of the intermolecular separation (Stryer and Haugland 1967), making it a sensitive technique for investigating a variety of biological phenomena that produce changes in molecular proximity (dos Remedios et al. 1987).

FRET measurement is mainly based on intensity, spectral or lifetime imaging (Jares-Erijman and Jovin 2003). Compared with intensity measurement, emission spectral imaging (ESI) and fluorescence lifetime imaging microscopy (FLIM) have been proved to be better options to quantify FRET efficiency (Pelet et al. 2006b). ESI, an imaging modality that allows for the accurate measurement of the abundance of fluorophores with overlapping emission spectra, is considered to be a comprehensive and photon-efficient method for imaging FRET efficiency in living cells (Thaler et al. 2005). FLIM, which relies on the measurement of temporally resolved fluorescence signal, is an advantageous means of determining FRET efficiency because it is independent of the fluorophore concentration (Zhang et al. 2005). Therefore, control measurements can be obtained from different cells for FLIM. Moreover the fluorescence decay offers additional information that can be used to calculate the relative fractions of free and associated donor molecules (Becker et al. 2004; Biskup et al. 2007), which is not available with any other intensity-based FRET measurements. The fluorescence lifetime detection technique based on time-correlated single-photon counting (TCSPC) are currently well implemented, with either single-photon (Becker et al. 2002) or two-photon excitation (TPE) (Bird et al. 2004). Two-photo excitation is more popularly used because of its advantage of reduced photo damage and therefore the ability of maintaining superior viability following prolonged exposure (Cheng et al. 2001; Squirrell et al. 1999; Zeng et al. 2006, 2007). Combining TPE-FLIM and TPE-ESI provides a powerful tool to obtain accurate data of FRET efficiency in the single living cells (Pelet et al. 2006a).

In an attempt to detect the caspase-3 activation in living cells, Miura et al. (Takemoto et al. 2003) constructed SCAT3, a FRET probe that consists of a donor (enhanced cyan fluorescent protein, ECFP) and an acceptor (Venus, a mutant of yellow fluorescent protein). The donor and acceptor are linked with a caspase-3 recognition and cleavage sequence (DEVD) (Takemoto et al. 2003; Wu et al. 2006a, b). The activated caspase-3 cleaves the linker DEVD, which induces a marked decrease of FRET efficiency and a significant increase of ECFP lifetime. Our previous studies of monitoring the spatial and temporal dynamics of caspase-3 activity were performed in a human lung cancer (ASTC-a-1) cell line stably expressing SCAT3 using FRET technique based on intensity measurement (Chen et al. 2007; Wang et al. 2005). In this study, we for the first time used both TPE-FLIM and ESI to study the caspase-3 activation inside the single living ASTC-a-1 cell stably expressing SCAT3 during taxol-, bufalin- and STS-induced PCD.

Materials and methods

Cell culture, transfection and screening

ASTC-a-1 cells, which were obtained from the Department of Medicine, Jinan University (Guangzhou, China), were cultured in Dulbecco's modified Eagle's medium (DMEM, Gibco, Grand Island, USA) supplemented with 10% fetal calf serum (FCS) (Sijiqing company, Hangzhou, China). Cell cultures were maintained at 37°C in a humidified 5% CO_2 incubator. After 24–48 h, the cells can be used for experiments.

Plasmid DNA of *SCAT3* was provided by Prof. Masayuki Miura (Takemoto et al. 2003), p*Bax-ECFP* and p*Bax-EYFP* were provided by Prof. Charles and Andrew (Valentijn et al. 2003). SCAT3, EYFP and ECFP were transfected into ASTC-a-1 cells respectively using Lipofectin

reagent (Carlsbad, CA). The cells stably expressing SCAT3 reporter were screened with 0.8 mg/ml G418, and positive clones were picked up with micropipettes (Wu et al. 2006a).

Assessment of cell viability

Cell viability after anticancer drug treatment was assessed by Counting Kit-8 (CCK-8, Dojindo, Japan) assay, according to the supplier recommendations. Absorbance was measured at 450 nm using auto microplate reader (infinite M200, Tecan, Austria). Cell viability was expressed as the percentage of viable cells relative to untreated cells using the absorbance at 450 nm, and then the inhibitory rate (R_I) was calculated: $R_I = [OD_{450}$ (control group) $- OD_{450}$ (drugged group)]/OD_{450} (control group) $\times$ 100%. All experiments were performed in quadruple on three separate occasions.

Detection of apoptosis

Apoptosis of cells was assessed by Hoechst33258/propidium iodide (PI) dual staining. Briefly, cells were grown on the coverslip of a chamber. After being washed with PBS three times, cells were stained with 10 μg/ml Hoechst33258 and 10 μg/ml PI for 20 min at 37°C in a humidified 5% CO_2 incubator. The cells were then washed three times with PBS and observed under a Zeiss Laser Scanning Confocal Microscope (LSM510, Zeiss, Germany). To measure the fluorescence of Hochest33342 (Ex352/Em461), the mercury lamp was used to excite Hochest33258 and a filter set (BP 365/12, FT 395, LP397) was inserted in the optical path. The BP 390–465 nm bandpass filter was used to record the emission fluorescence for the Hochest33342 channel. Hoechst staining images were acquired with a color CCD camera and PI staining images were acquired by confocal imaging.

Confocal fluorescence imaging and photobleaching of the acceptor of SCAT3

Fluorescence imaging and photobleaching of the receptor of FRET were performed using the Laser Scanning Confocal Microscope (LSM510/ConfoCor2, Zeiss, Germany). For FRET detection, 458 nm laser line from an Argon ion laser was used for ECFP excitation. Zeiss Plan-Neofluar 40×, NA = 1.45 oil immersion objective lens was used. Images were acquired through CFP and YFP filter channels respectively. Here, the filter sets used were CFP (band pass BP470–500 nm) and YFP (long-pass LP530 nm). 514 nm output from an Argon ion laser was used for photobleaching the receptor of SCAT3 Venus. The condition (37°C, 5% CO_2) was sustained during the measurement. All the quantitative analysis of the fluorescence images was performed using Zeiss Rel3.2 image processing software.

One-photon emission spectra detection

Cells stably expressing SCAT3 were cultured for 24 h in 96-well flat-bottomed microtiter plates at 5×10^5 per well in DMEM medium supplemented with 10% fetal calf serum. The emission spectra of the SCAT3 were detected by auto microplate reader (infinite M200, Tecan, Austria). The excitation wavelength of SCAT3 was 430 nm and the scanning range of fluorescence emission was from 456 to 600 nm, and the step size was 2 nm.

Two-photon excitation fluorescence spectral and lifetime imaging

TPE fluorescence imaging was performed using a Leica TCS SP2 Confocal Laser Scanning Microscope (Leica Microsystems Heidelberg GmbH, Mannheim, Germany). The output from a Ti:Sapphire femtosecond pulsed laser (Coherent Mira 900F, Coherent Inc., USA) is delivered into the microscope for TPE of the sample. The wavelength of the femtosecond laser was tuned to 780 nm for the excitation of the donor ECFP in the cells. In this work, a 40×/1.2 oil immersion fluorescence objective lens (Leica HC PLAN APO PH2) was used. For ESI, a wavelength scanning of the confocal microscope produced a stack of 2D x–y images at different emission wavelengths ranging from 450 to 600 nm, with each step being 5 nm. Fluorescence of ECFP was detected by a microchannel plate photomultiplier tube (MCP-PMT) (R3809U-50, Hamamatsu Photonics, Japan) and its lifetime was measured using a time-correlate single photon counting (TCSPC) module (SPC-150, Becker and Hickl GmbH, Germany). A bandpass filter was placed in front of the MCP-PMT for detecting fluorescence only from the ECFP. The FLIM data were processed using the SPCImage software by Becker & Hickl GmbH. For FLIM-FRET measurement, the fluorescence lifetime of the donor alone (τ_D) and also in the presence of the acceptor (τ_{DA}) were measured. If FRET occurs, τ_{DA} will be different from τ_D and this difference can be used to calculate FRET efficiency E as $E = 1 - \tau_{DA}/\tau_D$. The major advantage of FLIM is that it permits an internally calibrated measurement of FRET. Also, as only donor emission is monitored, factors that affect the quantum yield of the acceptor can be disregarded.

Statistics

Results were expressed as mean ± standard deviation (SD). Student's t test was used to compare the mean differences between samples using the statistical software SPSS

version 10.0 (SPSS, Chicago). Throughout the work, P values less than 0.05 were considered to be statistically significant. And all charts were drawn using software Origin version 6.0.

Results

Inhibition of cell viability by taxol, bufalin and STS

To investigate the cytotoxicity of taxol, bufalin and STS, ASTC-a-1 cells were treated with 70 μM taxol for 24 h, 0.1 μM bufalin for 48 h, and 1 μM STS for 12 h, respectively. Cell viability was assessed by CCK-8 assay. As is shown in Fig. 1a, the OD_{450} values for control and taxol, bufalin and STS treatment are 2.14 ± 0.0091, 0.70 ± 0.0976, 0.35 ± 0.0186 and 0.94 ± 0.0865, respectively. The inhibitory rates of ASTC-a-1 cells proliferation are corresponding to 0, 67.29, 83.64 and 56.07%, respectively. The results showed that ASTC-a-1 cells proliferation were significantly inhibited by taxol ($P < 0.001$), bufalin ($P < 0.001$) and STS ($P < 0.001$).

Figure 1b showed the confocal images of ASTC-a-1 cells after treatment with 70 μM taxol for 24 h, 0.1 μM bufalin for 48 h, and 1 μM STS for 6 h, respectively. Compared with control, cells treated with anticancer drugs showed shrinkage and ovalisation, and the nuclei condensation stained by Hoechst33258 was given in Fig. 1c. However, the cells were hardly stained by PI even in those strongly stained by Hoechst (data not shown), implying that the cell membrane was intact.

These data demonstrated that taxol, bufalin and STS induced cell death in PCD but not necrosis in the ASTC-a-1 cells.

Emission spectral analysis of caspse-3 activation inside single living cell after taxol, bufalin and STS treatment

ASTC-a-1 cells stably expressing SCAT3 were confirmed by both acceptor photobleaching and emission spectra assay, as described in our previous studies (Chen et al. 2007, 2008). Figure 2a gives the fluorescence images of two ASTC-a-1 cells stably expressing SCAT3 for the ECFP and Venus channels. SCAT3 distributed evenly in both nuclei and cytoplasm (Fig. 2a). The Venus in the rectangle area in Fig. 2a was selectively bleached by the maximal 514 nm laser. Compared with the cell (on right in Fig. 2a) without photobleaching, there was a marked decrease of intensity in Venus channel after bleaching, which coincided with an increase of ECFP (Fig. 2b). Furthermore, Fig. 2c shows one-photon emission spectrum of SCAT3 inside living cells excited by 430 nm light. Bimodal emission peaks of SCAT3 were observed around 476 or 526 nm, which is consistent with the previously published results (Chen et al.

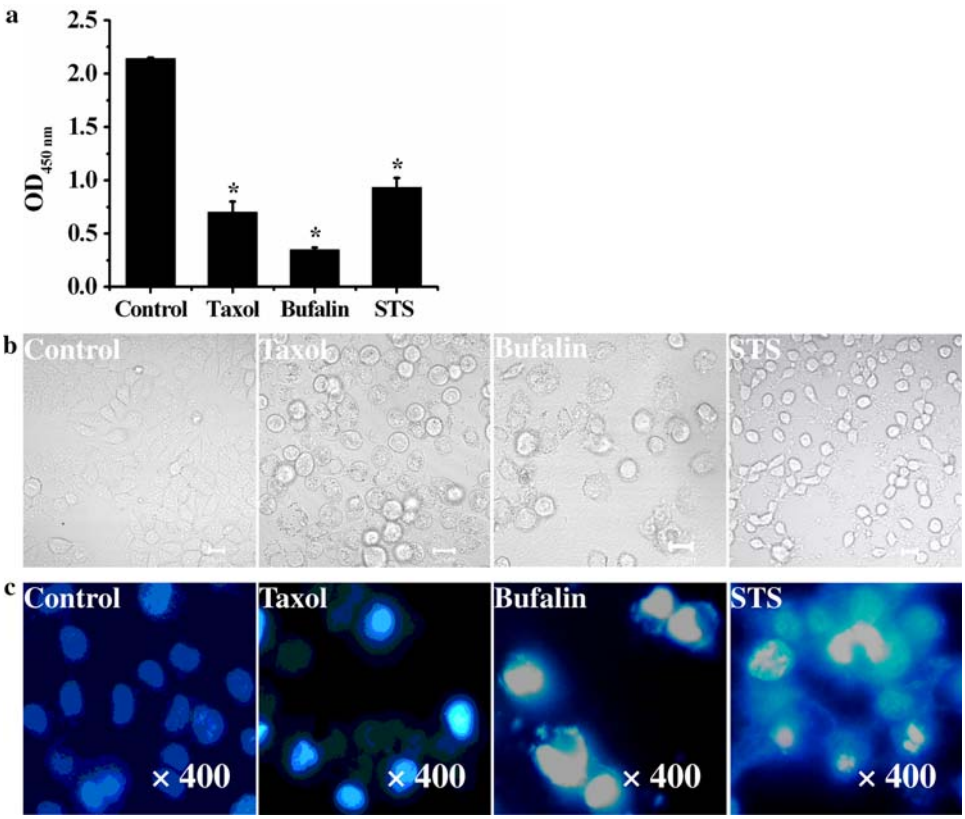

Fig. 1 Inhibition of taxol, bufalin and staurosporine (STS) on the cell viability. **a** OD_{450} values illustrating cell viability for the control, taxol, bufalin and STS treatment groups. The results are expressed as mean ± SD from at least four independent experiments. *$P < 0.001$ when compared with the control. **b** Confocal DIC images of cells for the control, taxol, bufalin and STS treatment. *Scale Bar* 20 μm. **c** Hochest33258 fluorescence images of cells for the control and taxol, bufalin and STS treatment. Magnification: ×400

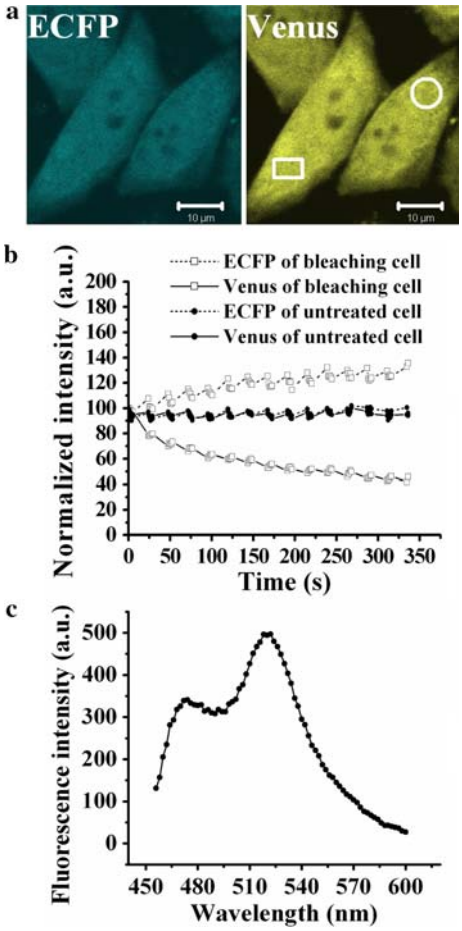

Fig. 2 ASTC-a-1 cells stably expressing SCAT3. **a** Confocal fluorescence images of ECFP and Venus channels for cells stably expressing SCAT3. *Scale bar* 10 μm. **b** Dynamics of the fluorescence intensity in both ECFP and Venus channels for the acceptor Venus photobleaching area (*rectangle area*) and the control without photobleaching (*circle area*) in Fig. 2a. All initial intensity is normalized to 100. **c** Emission spectra of SCAT3 in living cells excited with 406–436 nm

2008; Takemoto et al. 2003; Wang et al. 2008). These data confirmed that FRET exists between ECFP and Venus probes in the SCAT3 FRET reporter in living ASTC-a-1 cells.

Because of spectral overlap, the light used for the excitation of ECFP also excites Venus (Patterson et al. 2001). To lower this bleed-through, many studies offered various approaches to selectively excite ECFP with TPE wavelength, which was considered to be 785 nm by measuring the ratio of 535 to 480 nm emissions of cameleon at saturating calcium level in vitro (Fan et al. 1999). In this study, TPE emission spectra of SCAT3 inside the single living cell were acquired from twenty ASTC-a-1 cells stably expressing SCAT3 excited with 760, 770, 780, 790, 800, 810, 820 and 830 nm respectively. The ratio of 526 to 476 nm emissions did change with excitation wavelength, and reached the minimum at 780 nm (Fig. 3a), implying that 780 nm, which may selectively excite ECFP, is the optimal TPE wavelength for SCAT3. To further confirm the selective excitation of ECFP by 780 nm, we used 780 nm laser to excite the cells expressing EYFP-only which can be excited efficiently by 514 nm laser (Fig. 3b; upper panel), the emission in EYFP channel was hardly detected even using the maximum laser (Fig. 3b, lower panel). Thus the emission spectra for ECFP and SCAT3 were obtained using excitation with the 780 nm laser line in this study.

In order to confirm whether the autofluorescence of cells lead to a contamination for the detection upon excitation with 780 nm, the comparison of fluorescence intensity between a cell expressing ECFP-only and a similar cell not expressing ECFP was shown in Fig. 3c. The fluorescence intensity of a cell not expressing ECFP (Fig. 3c; Cell 1) is hardly detected compared with a similar cell expressing ECFP-only (Fig. 3c; Cell 2) at the same excitation conditions. These results show that the possibility of contamination by autofluorescence of cells can be excluded.

Representative emission spectra of ECFP from a living ASTC-a-1 cell expressing ECFP (Fig. 3d) is shown in Fig. 3e. Figure 3d also shows typical fluorescence images of some living cells stably expressing SCAT3 in absence and presence of the 1 μM STS for 6 h, 0.1 μM bufalin for 48 h, and 70 μM taxol for 24 h, respectively. The corresponding emission spectra of SCAT3 inside living cells in Fig. 3d are shown in Fig. 3e. Compared with the control, the emission peak at 526 nm disappeared but the emission increased markedly at 476 nm after STS or bufalin treatment. The emission ratio of 526 to 476 nm changed from 1.35 to 0.92 or 0.91, indicating that caspase-3 was activated during STS- or bufalin-induced apoptosis. In contrast, taxol treatment did not induce a significant change of SCAT3 spectra (Fig. 3e; taxol), suggesting that caspase-3 was not involved in taxol-induced PCD, which is in accordance with previously published results (Chen et al. 2008; Wang et al. 2008).

FLIM analysis of caspse-3 activation inside single living cell after taxol, bufalin and STS treatment

FLIM method was used to further confirm these observations. All samples were illuminated with femtosecond pulsed laser of 780 nm, which is the optimal wavelength for selectively exciting ECFP as described above. The fluorescence emission from ECFP was then selectively recorded using an interference filter (460–500 nm), as described in "Materials and methods". The same specimens were subsequently used for FLIM analysis after ESI. Figure 4a gives the FLIM images of cells expressing ECFP and SCAT3, respectively. Two typical time-resolved fluorescence decays (Fig. 4b; upper panel) corresponding to the pixels

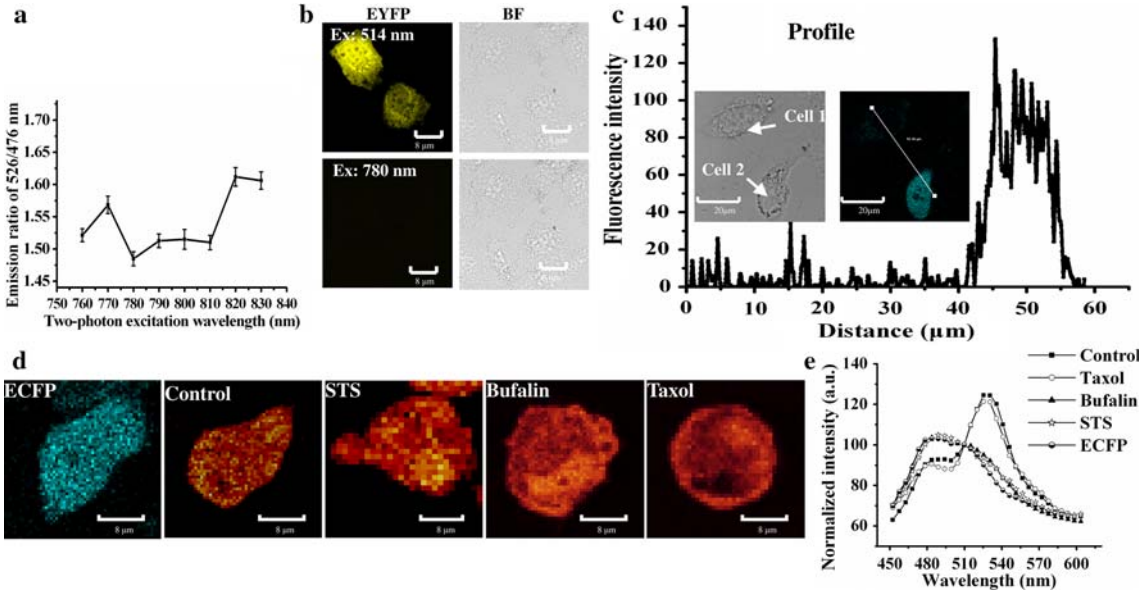

Fig. 3 Two-photon excitation (TPE) emission spectral analysis in single living ASTC-a-l cell. **a** Emission ratio of 526 to 476 nm in single living ASTC-a-l cells stably expressing SCAT3 with different TPE wavelength. The results are expressed as mean ± SD from total 20 cells in at least three independent experiments. **b** Confocal fluorescence images (EYFP channel) and BF images (BF channel) of the cells expressing EYFP only excited with 514 nm (*upper panel*) and 780 nm (*lower panel*) laser, respectively. *Scale bar* 8 μm. **c** A profile of the fluorescence intensity from a cell expressing ECFP-only (Cell 2) and a similar cell not expressing ECFP (Cell 1). Excitation wavelength: 780 nm. *Scale bar* 20 μm. **d** Confocal fluorescence images of the cell expressing ECFP and the cells stably expressing SCAT3 for the control, STS, bufalin and taxol treatment. *Scale bar* 8 μm. **e** Emission spectra of ECFP and SCAT3 inside single living cell corresponding to Fig. 3b. All intensity of the spectra at 510 nm is normalized to 100

marked by arrows in Fig. 4a were fitted using a single exponential decay model, which was good enough for photon data fitting (Fig. 4b; lower panel). The fluorescence decay profiles show that the lifetimes in cells expressing ECFP only and SCAT3 are quite different, which indicates that donor ECFP experience different excited state quenching mechanisms in cell expressing ECFP only (Fig. 4b; ECFP) and cell expressing SCAT3 (Fig. 4b; control). The ECFP lifetime histograms are shown in Fig. 4c, the mean fluorescence lifetime of ECFP over the whole cell expressing ECFP was 2.45 ns, which is consistent with previous results (Pepperkok et al. 1999; van Kuppeveld et al. 2002). In order to verify whether STS or Bufalin treatment lead to a change of the photophysics of ECFP, the lifetime of ECFP was measured in living cells expressing ECFP only after STS or Bufalin treatments, and the results showed that STS and Bufalin do not make a significant change of ECFP lifetime (data not shown). The lifetime of the donor ECFP in the cells stably expressing SCAT3 was 1.85 ns (Fig. 4c; control). STS or bufalin treatment induced the increase of the lifetime of donor ECFP from 1.85 to 2.21 or 2.01 ns (Fig. 4c; STS, bufalin). In contrast, taxol did not induce significant increase of fluorescence lifetime of ECFP (Fig. 4c; taxol). The fluorescence lifetimes of ECFP from 40 to 50 different cells in at least three independent experiments were listed in Table 1. The lifetime of the ECFP after taxol treatment was the same as that of the control (1.83 ± 0.02 ns). However, the lifetime of the donor ECFP significantly increased from 1.83 ± 0.02 to 2.05 ± 0.03 or 1.90 ± 0.03 ns after STS ($P = 0.001$) or bufalin ($P = 0.045$) treatment, and the FRET efficiency decreased from 24.38% (Control) to 15.29% (STS) or 21.49% (Bufalin). These results further demonstrated that caspase-3 was activated during STS- or bufalin-induced apoptosis, but was not involved in the taxol-induced PCD.

Discussion

Our results revealed that FRET based on FLIM and ESI analysis can be used to quantitatively monitor caspase-3 activation inside single living cells during anticancer drug-induced cell death. These results obtained from the FLIM and two-photo excitation ESI analysis are in accordance with previously published data of the caspase-3 activation using intensity and spectral analysis in living ASTC-a-1 cells stably expressing SCAT3 (Chen et al. 2007, 2008; Wang et al. 2005). However, intensity-based FRET signal is contaminated by donor crosstalk and acceptor bleed-through because of the spectral overlap. Many correction algorithms have been published to recover the FRET efficiency with good success, but they require multiple sets of images with varying excitation and detection conditions, as well as with reference samples that contain only one of

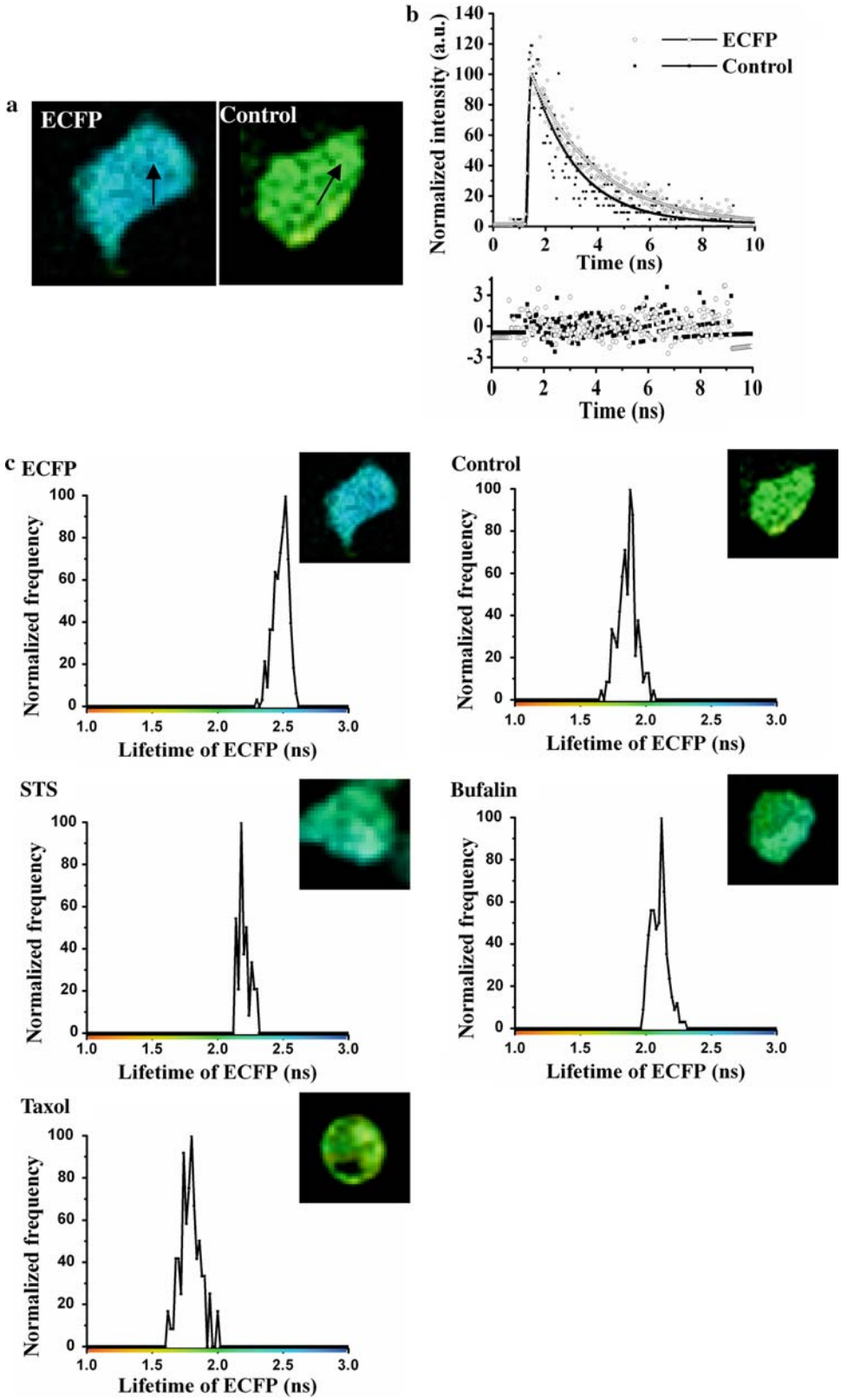

Fig. 4 FLIM analysis for ECFP in single living ASTC-a-1 cells. **a** FLIM images of the cells expressing ECFP and the cells stably expressing SCAT3. **b** Time-resolved fluorescence lifetime decays (*upper panel*) and the residuals (*lower panel*) of the fluorescence intensity of ECFP corresponding to the pixels marked by the *arrows* in Fig. 4a. **c** Histograms of the lifetimes of ECFP distribution for the whole cell expressing ECFP and that for the cells stably expressing SCAT3 for the control, taxol, bufalin and STS treatment

the fluorophore (Berney and Danuser 2003; Gordon et al. 1998; Xia and Liu 2001). In contrast, FLIM and ESI do not encounter such complex correction schemes (Clegg et al. 1993; Neher and Neher 2004), and they can be used to quantitatively obtain the FRET efficiency at single living cell level.

Table 1 Mean fluorescence lifetimes of ECFP and FRET efficiency by the FLIM analysis

Specimen[a]	$\tau \pm$ SD (ns)	E_{FRET} (%)
ECFP	2.42 ± 0.08	
Control	1.83 ± 0.02	24.38
STS	2.05 ± 0.03[b]	15.29[b]
Bufalin	1.90 ± 0.03[c]	21.49[c]
Taxol	1.83 ± 0.05	24.38

[a] ASTC-a-1 cell expressing ECFP and the cells stably expressing SCAT3 treatment with control, STS, bufalin and Taxol

[b] $P < 0.01$ when compared with the control

[c] $P < 0.05$ when compared with the control

ESI analysis has been widely used to measure FRET (Galvez et al. 2008; Thaler et al. 2005), and quantitative FRET efficiency can be calculated through spectral fitting method based on donor-acceptor pair emission spectra (Thaler et al. 2005). The spectral fitting method has the advantage of removing all the emission bleed-through and it is only required to selectively excite donor as efficiently as possible. To lower the acceptor bleed-through between ECFP and EYFP (Venus), it is necessary to verify which wavelength can selectively excite ECFP with TPE. Fan et al. 1999 found that the wavelength of 770–810 nm, especially at 785 nm, can selectively excite ECFP by measuring the ratio of 535 to 480 nm emissions of the calcium indicator cameleon at saturating calcium level in vitro. Cameleon, a calcium indicator based on FRET, consist of ECFP-CaM fused to M13-EYFP via a Gly–Gly spacer (Miyawaki et al. 1997). Venus, a variant of EYFP, is highly resistant to change in H^+ and Cl^- concentration in vitro and insensitive to environmental effects in living cells more than EYFP (Nagai et al. 2002). In this study, we measured the ratio of 526 to 476 nm emissions of SCAT3 in single living ASTC-a-1 cell stably expressing SCAT3 using TPE wavelengths from 760 to 830 nm, and found that 780 nm may selectively excite ECFP (Fig. 3a).

Our results also demonstrated that two-photon ESI could be used to analyze the caspase-3 activation in single living cell. Figure 2c graphically displays the emission spectra of SCAT3 inside living cells using auto microplate reader upon one-photon excitation with 406–436 nm light as in our previous study (Chen et al. 2008; Wang et al. 2008). For the bimodal emission peaks (Fig. 2c) to take place, two conditions had better to be met. First, there are more than 1×10^6 cells in each well of 96-well plate. Second, the transfection efficiency of *SCAT3* is more than 30%. Although this approach is widely used in our previous study (Chen et al. 2008; Wang et al. 2008), it is still hard to implement in single living cell study using confocal microscopy. Because one-photon excitation would require wavelengths of 430–440 nm, which are not available from the Argon ion or Krypton ion lasers most commonly found in confocal microscopes. Thus the tunable Ti: sapphire laser (typically 700–1,050 nm) is a universal replacement in TPE microscopy for all these separate one-photon excitation sources. Moreover, the near infrared light used for TPE is less harmful to living cells and generally has a better penetration in living tissues.

FLIM is considered to be one of the most reliable methods for FRET measurement in living cells (Suhling et al. 2005). Spectral fitting method can exclude the experimental artifact due to emission bleed-through and it has been proved to be good for ECFP–EYFP analysis (Thaler et al. 2005). However, it might be hampered with severe excitation spectral overlap existed in some FRET pairs. One main advantage of FLIM is that it could not be affected by excitation cross-talk, because FLIM-FRET only exploits the decrease of the donor lifetime with the efficiency of the energy transfer and the lifetime does not depend on the concentration of the fluorophores. It is necessary to selectively detect donor fluorescence using FLIM. In this study, the interference filter (460–500 nm) was used to selectively record the fluorescence emission from ECFP. The other main advantage of FLIM is that the FRET efficiency can be obtained from a single donor lifetime image (Table 1). These results demonstrated that FLIM was also available for caspase-3 activation analysis.

In this study, we for the first time used TPE FLIM and ESI to monitor caspase-3 activation inside single living ASTC-a-1 cell stably expressing SCAT3 during anticancer drug-induced cell death. These results demonstrated that caspase-3 was activated during STS- or bufalin-induced apoptosis, but was not involved in the taxol-induced PCD. Meanwhile, TPE FLIM and ESI analysis were also proved to be two valuable approaches for the detection of caspase-3 activation in single living cell.

Acknowledgments We wish to thank Prof. M. Miura for providing us with the *SCAT3* plasmid and Prof. Charles and Andrew for providing us with *Bax-ECFP* and *Bax-EYFP* plasmid. This study was supported by National Natural Science Foundation of China (Grant No. 30670507 and 60627003) and the Natural Science Foundation of Guangdong Province (F051001).

References

Andersson M, Sjöstrand J, Petersen A, Honarvar AKS, Karlsson J-O (2000) Caspase and proteasome activity during staurosporine-induced apoptosis in lens epithelial cells. Invest Ophthalmol Vis Sci 41:2623–2632

Becker W, Bergmann A, Biskup C, Zimmer T, Klöcker N, Benndorf K (2002) Multi-wavelength TCSPC lifetime imaging. Proc SPIE 4620:79–84. doi:10.1117/12.470679

Becker W, Bergmann A, Hink MA, König K, Benndorf K, Biskup C (2004) Fluorescence lifetime imaging by time-correlated single-photon counting. Microsc Res Tech 63:58–66. doi:10.1002/jemt.10421

Berney C, Danuser G (2003) FRET or no FRET: a quantitative study. Biophys J 84:3992–4010

Bird DK, Eliceiri KW, Fan C-H, White JG (2004) Simultaneous two-photon spectral and lifetime fluorescence microscopy. Appl Opt 43:5173–5182. doi:10.1364/AO.43.005173

Biskup C, Zimmer T, Kelbauskas L, Hoffmann B, Klöcker N, Becker W, Bergmann A, Benndorf K (2007) Multi-dimensional fluorescence lifetime and FRET measurements. Microsc Res Tech 70:442–451. doi:10.1002/jemt.20431

Chen T, Wang J, Xing D, Chen WR (2007) Spatio-temporal dynamic analysis of Bid activation and apoptosis induced by alkaline condition in human lung adenocarcinoma cell. Cell Physiol Biochem 20:569–578. doi:10.1159/000107540

Chen T, Wang X, Sun L, Wang L, Xing D, Mok M (2008) Taxol induces caspase-independent cytoplasmic vacuolization and cell death through endoplasmic reticulum (ER) swelling in ASTC-a-1 cells. Cancer Lett 270:164–172. doi:10.1016/j.canlet.2008.05.008

Cheng P, Lin B, Kao F, Gu M, Xu M, Gan X, Huang M, Wang Y (2001) Multi-photon fluorescence microscopy—the response of plant cells to high intensity illumination. Micron 32:661–669. doi:10.1016/S0968-4328(00)00068-8

Clegg RM, Murchie AI, Lilley DM (1993) The four-way DNA junction: a fluorescence resonance energy transfer study. Braz J Med Biol Res 26:405–416

Day TW, Najafi F, Wu CH, Safa AR (2006) Cellular FLICE-like inhibitory protein (c-FLIP): a novel target for taxol-induced apoptosis. Biochem Pharmacol 71:1551–1561. doi:10.1016/j.bcp.2006.02.015

dos Remedios CG, Miki M, Barden JA (1987) Fluorescence resonance energy transfer measurements of distances in actin and myosin: A critical evaluation. J Muscle Res Cell Motil 8:97–117. doi:10.1007/BF01753986

Fan GY, Fujisaki H, Miyawaki A, Tsay R-K, Tsien RY, Ellisman MH (1999) Video-rate scanning two-photon excitation fluorescence microscopy and ratio imaging with cameleons. Biophys J 76:2412–2420

Förster T (1948) Intermolecular energy migration and fluorescence. Ann Phys 6:55–75. doi:10.1002/andp.19484370105

Galvez EM, Zimmermann B, Rombach-Riegraf V, Bienert R, Gräber P (2008) Fluorescence resonance energy transfer in single enzyme molecules with a quantum dot as donor. Eur Biophys J. doi:10.1007/s00249-008-0351-7

Gordon GW, Berry G, Liang XH, Levine B, Herman B (1998) Quantitative fluorescence resonance energy transfer measurements using fluorescence microscopy. Biophys J 74:2702–2713

Green DR (1998) Apoptotic pathways: the roads to ruin. Cell 94:695–698. doi:10.1016/S0092-8674(00)81728-6

Huisman C, Ferreira CG, Bröker LE, Rodriguez JA, Smit EF, Postmus PE, Kruyt FAE, Giaccone G (2002) Paclitaxel triggers cell death primarily via caspase-independent routes in the non-small cell lung cancer cell line NCI-H460. Clin Cancer Res 8:596–606

Jares-Erijman EA, Jovin TM (2003) FRET imaging. Nat Biotechnol 21:1387–1395. doi:10.1038/nbt896

Kerr JF, Winterford CM, Harmon BV (1994) Apoptosis: its significance in cancer and cancer therapy. Cancer 73:2013–2026. doi:10.1002/1097-0142(19940415)73:8<2013::AID-CNCR2820730802>3.0.CO;2-J

Lin J, Zhang Z, Zeng S, Zhou S, Liu B, Liu Q, Yang J, Luo Q (2006) TRAIL-induced apoptosis proceeding from caspase-3-dependent and -independent pathways in distinct HeLa cells. Biochem Biophys Res Commun 346:1136–1141. doi:10.1016/j.bbrc.2006.05.209

Ling Y-H, Zhong Y, Roman P-S (2001) Disruption of cell adhesion and caspase-mediated proteolysis of β- and γ-Catenins and APC protein in raclitaxel-induced apoptosis. Mol Pharmacol 59:593–603

Lu K-H, Lue K-H, Liao H-H, Lin K-L, Chung J-G (2005) Induction of caspase-3-dependent apoptosis in human leukemia HL-60 cells by paclitaxel. Clin Chim Acta 357:65–73. doi:10.1016/j.cccn.2005.02.003

Masuda Y, Kawazoe N, Nakajo S, Yoshida T, Kuroiwa Y, Nakaya K (1995) Bufalin induces apoptosis and influences the expression of apoptosis related genes in human leukemia cells. Leuk Res 19:549–556. doi:10.1016/0145-2126(95)00031-I

Miyawaki A, Llopis J, Heim R, McCaffery JM, Adams JA, Ikura M, Tsien RY (1997) Fluorescent indicators for Ca^{2+} based on green fluorescent proteins and calmodulin. Nature 388:882–887. doi:10.1038/42264

Nagai T, Ibata K, Park ES, Kubota M, Mikoshiba K, Miyawaki A (2002) A variant of yellow fluorescent protein with fast and efficient maturation for cell-biological applications. Nat Biotechnol 20:87–90. doi:10.1038/nbt0102-87

Neher RA, Neher E (2004) Applying spectral fingerprinting to the analysis of FRET images. Microsc Res Tech 64:185–195. doi:10.1002/jemt.20078

Ofir R, Seidman R, Rabinski T, Krup M, Yavelsky V, Weinstein Y, Wolfson M (2002) Taxol-induced apoptosis in human SKOV3 ovarian and MCF7 breast carcinoma cells is caspase-3 and caspase-9 independent. Cell Death Differ 9:636–642. doi:10.1038/sj.cdd.4401012

Patterson G, Day RN, Piston D (2001) Fluorescent protein spectra. J Cell Sci 114:837–838

Pelet S, Previte MJR, Kim D, Kim KH, Su T-TJ, So PTC (2006a) Frequency domain lifetime and spectral imaging microscopy. Microsc Res Tech 69:861–874. doi:10.1002/jemt.20361

Pelet S, Previte MJR, So PTC (2006b) Comparing the quantification of Förster resonance energy transfer measurement accuracies based on intensity, spectral, and lifetime imaging. J Biomed Opt 11:034017. doi:10.1117/1.2203664

Pepperkok R, Squire A, Geley S, Bastiaens PI (1999) Simultaneous detection of multiple green fluorescent proteins in live cells by fluorescence lifetime imaging microscopy. Curr Biol 9:269–272. doi:10.1016/S0960-9822(99)80117-1

Rehm M, Düßmann H, Jänicke RU, Tavaré JM, Kögel D, Prehn JH (2002) Single cell fluorescence resonance energy transfer analysis demonstrates that caspase activation during apoptosis is a rapid process. Role of caspase-3. J Biol Chem 277:24506–24514. doi:10.1074/jbc.M110789200

Rosales T, Georget V, Malide D, Smirnov A, Xu J, Combs C, Knutson JR, Nicolas J-C, Royer CA (2007) Quantitative detection of the ligand-dependent interaction between the androgen receptor and the co-activator, Tif2, in live cells using two color, two photon fluorescence cross-correlation spectroscopy. Eur Biophys 36:153–161. doi:10.1007/s00249-006-0095-1

Salako MA, Carter MJ, Kass GEN (2006) Coxsackievirus protein 2BC blocks host cell apoptosis by inhibiting caspase-3. J Biol Chem 281:16296–16304. doi:10.1074/jbc.M510662200

Shajahan AN, Wang A, Decker M, Minshall RD, Liu MC, Clarke R (2007) Caveolin-1 tyrosine phosphorylation enhances paclitaxel-mediated cytotoxicity. J Biol Chem 282:5934–5943. doi:10.1074/jbc.M608857200

Son Y-O, Choi K-C, Lee J-C, Kook S-H, Lee S-K, Takada K, Jang Y-S (2006) Involvement of caspase activation and mitochondrial stress in taxol-inducedapoptosis of Epstein–Barr virus-infected Akata cells. Biochim Biophys Acta 1760:1894–1902

Squirrell JM, Wokosin DL, White JG, Bavister BD (1999) Long-term two-photon fluorescence imaging of mammalian embryos without compromising viability. Nat Biotechnol 17:763–767. doi:10.1038/11698

Stryer L, Haugland R (1967) Energy transfer: a spectroscopic ruler. Proc Natl Acad Sci USA 58:719–726. doi:10.1073/pnas.58.2.719

Suhling K, French PMW, Phillips D (2005) Time-resolved fluorescence microscopy. Photochem Photobiol Sci 4:13–22. doi:10.1039/b412924p

Sun XM, MacFarlanc M, Zhuang J, Wolf BB, Green DR, Cohen GM (1999) Distinct caspase cascades are initiated in receptor-mediated and chemical-induced apoptosis. J Biol Chem 274:5053–5060. doi:10.1074/jbc.274.8.5053

Takemoto K, Nagai T, Miyawaki A, Miura M (2003) Spatio-temporal activation of caspase revealed by indicator that is insensitive to environmental effects. J Cell Biol 160:235–243. doi:10.1083/jcb.200207111

Thaler C, Koushik SV, Blank PS, Vogel SS (2005) Quantitative multiphoton spectral imaging and its use for measuring resonance energy transfer. Biophys J 89:2736–2749. doi:10.1529/biophysj.105.061853

Valentijn AJ, Metcalfe AD, Kott J, Streuli CH, Gilmore AP (2003) Spatial and temporal changes in Bax subcellular localization during anoikis. J Cell Biol 162:599–612. doi:10.1083/jcb.200302154

van Kuppeveld FJ, Melchers WJ, Willems PH, Gadella TW Jr (2002) Homomultimerization of the coxsackievirus 2B protein in living cells visualized by fluorescence resonance energy transfer microscopy. J Virol 76:9446–9456. doi:10.1128/JVI.76.18.9446-9456.2002

Wan Q, Liu L, Xing D, Chen Q (2008) Bid is required in NPe6-PDT-induced apoptosis. Photochem Photobiol 84:250–257

Wang F, Chen T, Xing D, Wang J, Wu Y (2005) Measuring dynamics of caspase-3 activity in living cells using FRET technique during apoptosis induced by high fluence low power laser irradiation. Lasers Surg Med 36:2–7. doi:10.1002/lsm.20130

Wang X, Chen T, Sun L, Cai J, Wu M, Mok M (2008) Live morphological analysis of taxol-induced cytoplasmic vacuoliazation in human lung adenocarcinoma cells. Micron. doi:10.1016/j.micron.2008.04.007

Watabe M, Ito K, Masuda Y, Nakajo S, Nakaya K (1998) Activation of AP-1 is required for bufalin-induced apoptosis in human leukemia U937 cells. Oncogene 16:779–787. doi:10.1038/sj.onc.1201592

Wu Y, Xing D, Chen WR (2006a) Single cell FRET imaging for determination of pathway of tumor cell apoptosis induced by photofrin-PDT. Cell Cycle 5:729–734

Wu Y, Xing D, Luo S, Tang Y, Chen Q (2006b) Detection of caspase-3 activation in single cells by fluorescence resonance energy transfer during photodynamic therapy induced apoptosis. Cancer Lett 235:239–247. doi:10.1016/j.canlet.2005.04.036

Wu Y, Xing D, Chen WR, Wang X (2007) Bid is not required for Bax translocation during UV-induced apoptosis. Cell Signal 19:2468–2478. doi:10.1016/j.cellsig.2007.07.024

Xia Z, Liu Y (2001) Reliable and global measurement of fluorescence resonance energy transfer using fluorescence microscopes. Biophys J 81:2395–2402

Xue LY, Chiu SM, Oleinick NL (2003) Staurosporine-induced death of MCF-7 human breast cancer cells: distinction between caspase-3-dependent steps of apoptosis and the critical lethal lesions. Exp Cell Res 283:135–145. doi:10.1016/S0014-4827(02)00032-0

Yeh J-Y, Huang WJ, Kan S-F, Wang PS (2003) Effects of bufalin and cinobufagin on the proliferation of androgen dependent and independent prostate cancer cells. Prostate 54:112–124. doi:10.1002/pros.10172

Zeng S, Lu X, Zhan C, Chen WR, Xiong W, Jacuqes SL, Luo Q (2006) Simultaneous compensation for spatial and temporal dispersion of acousto-optical deflectors for two-dimensional scanning with a single prism. Opt Lett 31:1091–1093. doi:10.1364/OL.31.001091

Zeng S, Li D, Liu J, Luo Q (2007) Pulse broadening of the femtosecond pulses in a Gaussian beam passing an angular disperser. Opt Lett 32:1180–1182. doi:10.1364/OL.32.001180

Zhang J, Xing D, Gao X (2008) Low-power laser irradiation activates Src tyrosine kinase through reactive oxygen species-mediated signaling pathway. J Cell Physiol 217:518–528. doi:10.1002/jcp.21529

Zhang S, Wang G, Fernig DG, Rudland PS, Webb SED, Barraclough R, Martin-Fernandez M (2005) Interaction of metastasis-inducing S100A4 protein in vivo by fluorescence lifetime imaging microscopy. Eur Biophys J 34:19–27. doi:10.1007/s00249-004-0428-x